Int. J. Electrochem. Sci., 11 **(2016)** 8391 – 8404, doi: 10.20964/2016.10.39

International Journal of
ELECTROCHEMICAL
SCIENCE
www.electrochemsci.org

An RDE Research on the Preparation Process of β-PbO_2-CoO_x Composite Coatings

Sha Han[1], *Shiwei He*[1], *Ruidong Xu*[1,2,*], *Jiong Wang*[1], *Buming Chen*[1]

[1]Faculty of Metallurgical and Energy Engineering, Kunming University of Science and Technology, Kunming 650093, China
[2]State Key Laboratory of Complex Nonferrous Metal Resources Clean Utilization, Kunming 650093, China
[*]E-mail: rdxupaper@aliyun.com

Received: 28 June2016/ *Accepted:* 5 August 2016 / *Published:* 6 September 2016

The electrosynthesis of cobalt-doped lead dioxide in an acidity bath has been studied using PARSTAT2273 electrochemical workstation with rotating disk electrode (RDE) and β (Beta)-PbO_2-CoO_x composite coatings were obtained by means of anodic galvanostatic polarization. The concentrations of Co^{2+} and Pb^{2+}, pH, temperature and rotation velocity of the electrode effects on deposition behavior have been investigated. The amounts of PbO_2 deposited on the electrode surface increase with increasing concentrations of Co^{2+}, Pb^{2+}, H^+ and temperature within a certain range. There are only one main peak oxide peak ($Pb^{2+}\rightarrow PbO_2$) and reduction peak ($PbO_2\rightarrow Pb^{2+}$) with both anodic and cathodic scan in the cyclic voltammetry curves. The steady-state measurements show that the most suitable deposition current density is 6 mA/cm^2. Surface analysis by SEM and XRD reveals that the Co-doped PbO_2 has more uniform morphology and smaller crystals size than pure PbO_2. The E-t curves show that Co^{2+} added into the original plating bath brings on a large amounts of nucleation points for β-PbO_2 deposition.

Keywords:β-PbO_2, RDE, Cobalt, Composite coating, Electrosynthesis

1. INTRODUCTION

Lead dioxide possesses good electrical conductivity, low cost, excellent corrosion resistance and good electro-catalytical capabilities [1], and it is usually used as insoluble anode in electrochemical processes, such as preparation of ozone [2,3], analytical sensors [4], waste water treatment [5-8], lead-acid cell [9,10] and electrowinning process [11]. The α (Alpha)-PbO_2 and β (Beta)-PbO_2 are two allotropes of lead dioxide, and β-PbO_2 has a tetragonal rutile structure, which is compact and has better conductivity than α-PbO_2 [12,13]. To the best of our knowledge, the performance of the surfactant layer β-PbO_2 is still not satisfactory. Therefore, some researchers make

β-PbO_2 co-doped with other substance in order to improve the surface microstructures, reduce the brittleness and distortion, and ameliorate the catalytic activity [14].

Cobalt is in the fourth cycle of the periodic table of elements, belongs to the Ⅷ family and has catalytic effect by forming the stable oxides on the anode surfaces [15]. A cobalt-doped lead dioxide electrode was prepared by electrodeposition, which has a higher electro-catalytic activity than undoped samples [16]. Doping Co in lead dioxide has the effect of promoting oxygen evolution [17]. A.B. Velichenko etc., who took an investigation of cobalt-doped lead dioxide, which aimed at producing anodes with improved electrocatalytic acitity and stability, and found parameters affecting the amount of Co that is incorporated into PbO_2 films [18].

The conditions (mainly composition and temperature of the synthesizing bath) used for the electrodeposition have a significant effect on the properties and reactivity of the resulting films. Cyclic voltammetry paired with a rotating disk electrode has been employed for studying surface adsorption, deposition and the kinetics of charge transfer [19-25]. In this present work, the effects of different parameters on electrodeposition of Co-doped lead dioxide in acidity solutions are studied by cyclic voltammetry and RDE. The phase compositions and surface microstructures of PbO_2 layers were examined by means of X-ray diffractometer (XRD) and scanning electron microscopy (SEM). These research results are helpful to provide the theoretical basis and technical support for the preparation of co-doped lead dioxide from the bath.

2. EXPERIMENTS

An electrochemical workstation (PARSTAT2273) and RDE with a three-electrode system were used for testing cyclic voltammetry curves and steady-state polarization curves, which is also used to synthesize the β-PbO_2-CoO_x composite coatings and measure the deposition potential of the deposits. RDE with an exposed Pt was the working electrode, the saturated calomel electrode (SCE) was used as the reference electrode, the counter electrode was platinum sheet, the working electrode and the reference electrode were linked through the Luggin capillary filled with agar and potassium chloride. The distance between the reference electrode and the working electrode was about 4 times of the diameter of capillary. The Co content in the β-PbO_2-CoO_x composite coatings was measured by inductively coupled plasma optical emission spectrometer (ICP-OES). All potentials given in the research are against SCE.

Acid bath compositions for testing cyclic voltammetry were the following as: 0~300 g/L $Pb(NO_3)_2$, 5~25 g/L HNO_3, 0~50 g/L $Co(NO_3)_2 \cdot 6H_2O$. All chemicals are of reagent grade. The conditions of testing cyclic voltammetry curves were the following as: scan rate is 50 mv/s, potential window 0~2 V. The solutions for preparing anode material deposition and testing steady-state polarization curves were the following as: 200 g/L $Pb(NO_3)_2$, 15 g/L HNO_3, 30 g/L $Co(NO_3)_2 \cdot 6H_2O$. The samples were prepared at a constant current density with 6 mA/cm^2 at 30 ℃ for 2 hour. The morphological and phase composition of the samples were measured by scanning electron microscope and X-ray diffractometer, respectively. The voltage range for testing steady-state polarization curves is 1.3 V~1.8 V, the testing temperature is 30 ℃.

3. RESULTS AND DISCUSSION

3.1. Cyclic voltammetry study

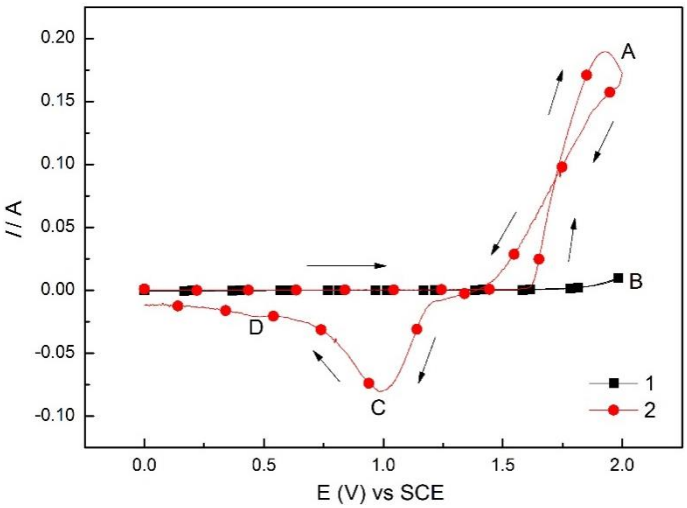

Figure 1. Cyclic voltammetry curves for the Pt-RDE in solutions: (1) 15 g/L HNO_3; (2) 15 g/L HNO_3+250 g/L $Pb(NO_3)_2$. v = 50 mV/s

Cyclic voltammetry curves for the Pt-RDE in the solution of 15 g/L HNO_3+250 g/L $Pb(NO_3)_2$ and blank solution (15 g/L HNO_3) are shown in Fig. 1. Only one peak is observed at E_B=2.0 V in the blank curve, which corresponds to the oxygen evolution. when Pb^{2+} is added to the solution, there is an anodic peak at E_A=1.9 V. Comparing peaks A and B, the intensity of peak A is much stronger than peak B, this could be explained by the existence of simultaneous reactions of PbO_2 formation and oxygen evolution in peak A [26]. At E_C=0.5 V and E_D=1.0 V, there are two cathodic peaks, corresponding to the PbO_2 reduction process. The reduction process could be explained by Formula 3 [27]. Two cathodic current peaks correspond to the reduction process of two crystal lead dioxide (β-form and α-form) [28], peak C represents β-PbO_2 and peak D represents α-PbO_2.

$$PbO_2 + 4H^+ + 2e = Pb^{2+} + 2H_2O \qquad (1)$$

Cyclic voltammetry curves for the Pt-RDE in the presence of Pb^{2+}, with or without Co^{2+} at 35 ℃, are shown in Fig. 2. On the anodic branch of the curve, only one peak can be observed at the potential 2.0 V. On the cathodic branch of the curve, one peak (C and D) can be detected in the potentials range of 0.75~1.25 V. The appearance of peak B is different from peak A. The intensity of peak A is stronger than peak B probably due to oxygen evolution acceleration by Co^{2+} in the solution. The area and the magnitude I_p of the reduction peak are a good measure of the rate and quantity of PbO_2 deposition on the electrode surface [29]. The intensity of peak D is stronger than peak C, indicating that the deposition amount of PbO_2 through the anodic scan process is larger in the Co^{2+} containing solution. The conclusion can be drawn that Co^{2+} in the solution can promote the formation of the PbO_2.

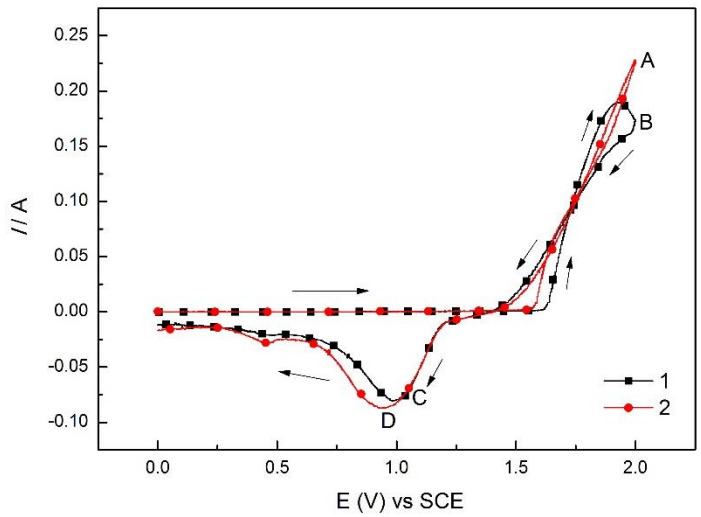

Figure 2. Cyclic voltammetry curves for the Pt-RDE in solutions: (1) 15 g/LHNO_3+250 g/L $Pb(NO_3)_2$; (2) 15 g/L HNO_3+250 g/L $Pb(NO_3)_2$+20 g/L $Co(NO_3)_2{\cdot}6H_2O$. v = 50 mV/s

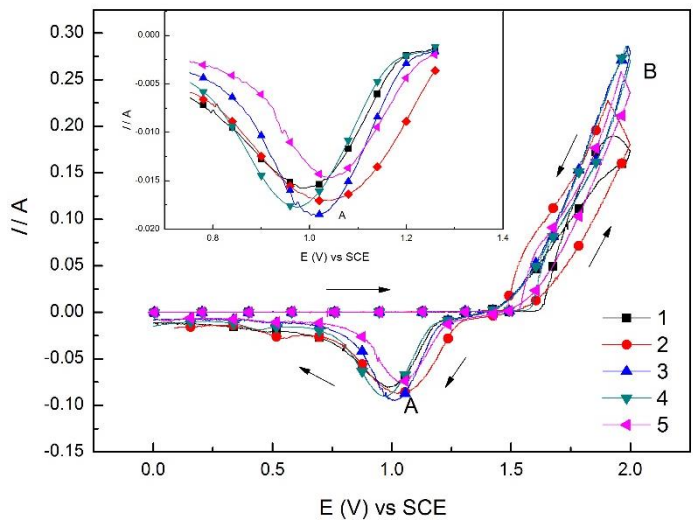

Figure 3. Cyclic voltammetry curves for the Pt-RDE in the solution 15 g/L HNO_3+250g/L $Pb(NO_3)_2$+0~50 g/L $Co(NO_3)_2{\cdot}6H_2O$: (1) 0 g/L ; (2) 20 g/L ; (3) 30 g/L ; (4) 40 g/L ; (5) 50 g/L ; v = 50 mV/s

Fig.3 shows the Cyclic voltammetry curves for the Pt-RDE in solution containing different $Co(NO_3)_2{\cdot}6H_2O$ concentration ($Pb(NO_3)_2$ and HNO_3 controlled at 250 g/L and 15 g/L) with a scan rate of 50 mV/s at 35 ℃. On the anodic branch of curve, only one peak can be observed at the potential 2.0 V. The intensity of peak B is affected by the mixed influence of Pb^{2+} oxidation process and oxygen evolution [26,30]. The illustration is an enlarged view of the cathodic branch of the cyclic voltammetry curves. On the cathodic branch of the curve, the intensity of peak A increases as the $Co(NO_3)_2{\cdot}6H_2O$ concentration increases from 0 to 30 g/L. And the intensity of cathodic current peak is strongest when $Co(NO_3)_2{\cdot}6H_2O$ concentration reaches to 30 g/L. However, the further increasing of the $Co(NO_3)_2{\cdot}6H_2O$ concentration leads to the intensity decrease of the peak A within the $Co(NO_3)_2{\cdot}6H_2O$

concentration range of 30~50 g/L. When the concentration of $Co(NO_3)_2 \cdot 6H_2O$ increases from 0 to 30 g/L, the exiting of Co^{2+} in the original plating solution accelerate the rate of the β-PbO_2 deposition process. When the concentration of $Co(NO_3)_2 \cdot 6H_2O$ increases from 30 to 50 g/L, the amount of CoO_x deposition in the electrode surface increases, which leads to oxygen evolution acceleration [18]. The oxygen evolution and β-PbO_2 deposition are two competitive processes [31-34]. So the enhanced oxygen evolution reaction hinder β-PbO_2 deposition process give rise to the amount of β-PbO_2 deposition decrease.

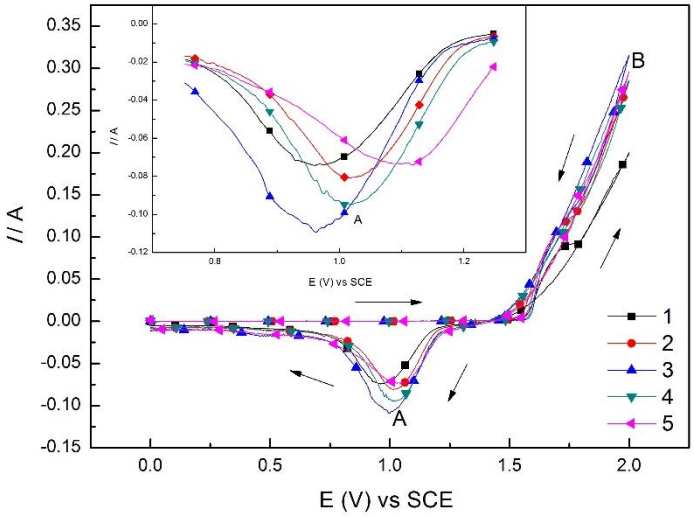

Figure 4. Cyclic voltammetry curves for the Pt-RDE in the solution 15g/L HNO_3+30 g/L $Co(NO_3)_2 \cdot 6H_2O$+100~300 g/L $Pb(NO_3)_2$: (1) 100 g/L；(2) 150 g/L；(3) 200 g/L；(4) 250 g/L；(5) 300 g/L；v = 50 mV/s

Fig.4 shows the Cyclic voltammetry curves for the Pt-RDE in solution containing different $Pb(NO_3)_2$ concentration ($Co(NO_3)_2 \cdot 6H_2O$ and HNO_3 controlled at 30 g/L and 15 g/L) with a scan rate of 50 mV/s at 35 ℃. The intensity of peak A at about E=1.0 V increases as $Pb(NO_3)_2$ concentration increases, and the intensity of cathodic peak A is strongest when $Pb(NO_3)_2$ concentration reaches to 200 g/L. A further increasing $Pb(NO_3)_2$ concentrations from 200 g/L to 300 g/L in the original plating bath, leads to the decreasing of the intensity of peak A at about E=1.0 V. In conclusion, the rate of β-PbO_2 deposition increasesas with $Pb(NO_3)_2$ concentration within a certain range (0~200g/L). Pb^{2+} ions decreases when $Pb(NO_3)_2$ concentration is less than 200 g/L, which cause the decreasing of the PbO_2 deposition rate. 15 g/L HNO_3 can inhibit the hydrolysis of Pb^{2+} ions completely when the $Pb(NO_3)_2$ concentration is 200 g/L. When the concentration of $Pb(NO_3)_2$ increases from 200 to 300 g/L, the increasing of $Pb(NO_3)_2$ concentration leads to the increasing of lead-acid ratio. The increased lead-acid ratio could cause part of Pb^{2+} hydrolyze to micro soluble substance $Pb(OH)_2$, according to the equation (2). In this case, the decreasing of free Pb^{2+} give rise to slower the rate of the β-PbO_2 deposition process.

$$Pb^{2+} + 2H_2O = Pb(OH)_2 \downarrow + 2H^+ \qquad (2)$$

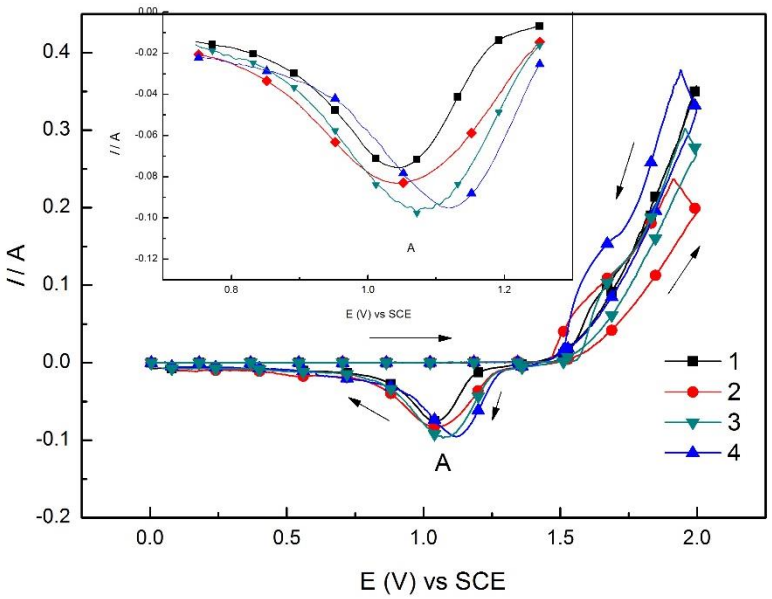

Figure 5. Cyclic voltammetry curves for the Pt-RDE in the solution 5~25 g/L HNO_3+30 g/L $Co(NO_3)_2 \cdot 6H_2O$+200 g/L $Pb(NO_3)_2$: (1) 5 g/L ; (2) 10 g/L ; (3) 15 g/L ; (4) 20 g/L ; v = 50 mV/s

Fig.5 shows the Cyclic voltammetry curves for the Pt-RDE in solution containing different HNO_3 concentration ($Co(NO_3)_2 \cdot 6H_2O$ and $Pb(NO_3)_2$ controlled at 30 g/L and 200 g/L) with a scan rate of 50 mV/s at 35 ℃. As can be seen, the magnitude I_p of peak A at about E=1.0 V increases as HNO_3 concentration increases on the illustration of the negative branch of the cyclic voltammetry curves, $Pb(NO_3)_2$ in the solution could hydrolyze to micro soluble substance $Pb(OH)_2$, which can be got from reaction (2). HNO_3 (H^+) in the solution could inhibit the hydrolyztion of Pb^{2+}, the hydrolysis degree of Pb^{2+} will gradually decrease with the increasing of the HNO_3 concentration in the bath. In this case, Pb^{2+} could be oxidized to lead dioxide, according to the increasing amount of β-PbO_2 electrodeposition.

The potential of peak A shifted slightly to a more positive potential as the HNO_3 concentration increased. One can observe the intensity of peak A obtained at the HNO_3 concentration of 15 g/L and 20 g/L are very close. But they doesn't coincide in the potential. The potential of peak A of curve 4 is more positive. This phenomenon is caused by the increasing of free H^+ in the bath as HNO_3 concentration continuously increases, which leads to the faster dissolution rate of the deposited PbO_2. As a result, the further positive potential of peak A is occurred. In addition, a rise of the HNO_3 concentration would bring about an increase of Co content and a decrease of the electrodeposition potential, which were studied by S. Cattarin [16] and A.B. Velichenko [18].

Fig.6 shows the cyclic voltammetry curves of the solution (200 g/L $Pb(NO_3)_2$, 15 g/L HNO_3 and 30 g/L $Co(NO_3)_2 \cdot 6H_2O$) at different temperatures. The transformation of peak A intensity has two stages: firstly, peak A increases with the temperature until the temperature reaches 30 ℃, indicating that the reaction of the lead dioxide deposition is promoted by temperature in the range of 20~30 ℃. Secondly, the intensity of peak A decreases follows the temperature range of 30~45 ℃, this happens because the lead dioxide deposition is an exothermic reaction and higher temperature can inhibit the β-

PbO_2 deposition [27]. As a result, the continual increasing of temperature will hinder Pb^{2+} from oxidizing and synthesizing β-PbO_2. In addition, in order to prevent Pb(II) ions hydrolysisand improve deposition of β-PbO_2, the suitable temperature for β-PbO_2 deposition is 30 ℃。

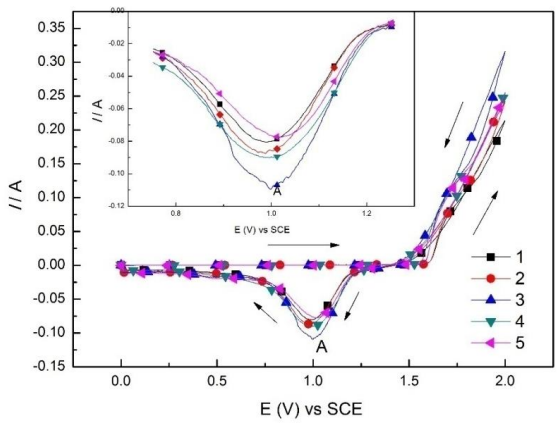

Figure 6. Cyclic voltammetry curves for the Pt-RDE of different bath temperatures in the solution 15 g/L HNO_3+30 g/L $Co(NO_3)_2 \cdot 6H_2O$+200 g/L $Pb(NO_3)_2$: (1) 20 ℃ ; (2) 25 ℃ ; (3) 30 ℃ ; (4) 35 ℃ ; (5) 40 ℃ ; v = 50 mV/s.

3.2. Rate-determining step

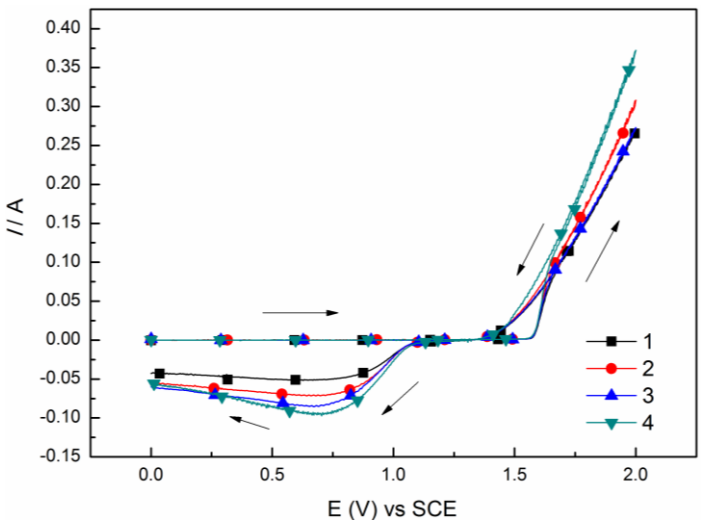

Figure 7. Cyclic voltammetry curves for the Pt-RDE in the solution of 15 g/L HNO_3+30 g/L $Co(NO_3)_2 \cdot 6H_2O$+200 g/L $Pb(NO_3)_2$. Rotation velocity of electrode/rev min^{-1}: (1) 300 ; (2) 600 ; (3) 900 ; (4) 1200; v = 50 mV/s

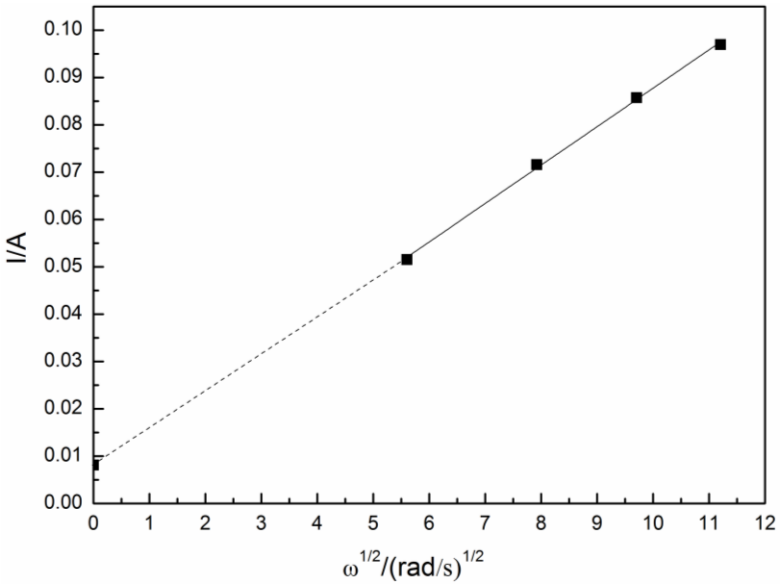

Figure 8. Levich plot of anodic currents for β-PbO_2-CoO_x films deposition on Pt disk in the solution of 15 g/L HNO_3+30 g/L $Co(NO_3)_2 \cdot 6H_2O$+200 g/L $Pb(NO_3)_2$

Fig. 7 shows Cyclic voltammetry curves for the Pt-RDE in the solution of 15 g/L HNO_3+30 g/L $Co(NO_3)_2 \cdot 6H_2O$+200 g/L $Pb(NO_3)_2$ at Rotation velocity of electrode. Fig. 8 shows the fitting results of the reduction peak current *I* (cathodic peak on the cyclic voltammetry curves in Fig. 7) on $\omega^{1/2}$ (the square root of the electrode rotating angular speed) by the Levich equation ($I=0.62nFAD^{2/3}v^{-1/6}C\omega^{1/2}$).

As can be seen from Fig. 7, the intensity of cathodic peak increases as electrode rotation speed grows due to the increasing of PbO_2 deposition amount at 30 ℃. Because the peak potential of PbO_2 deposition and oxygen evolution are very close for nitrate solution, it is diffcult to exclude the influence of oxygen evolution on the PbO_2 deposition current though the anodic scan. Therefore, using the reduction peak ($PbO_2 \rightarrow Pb^{2+}$) current instead of oxide peak ($Pb^{2+} \rightarrow PbO_2$) current [18,29,33,34]. As can be seen from Fig. 8, the dependence of the cathodic current density on the square root of the electrode rotation rate is linear and the coefficient of determination R^2 is 0.99839, indicating that it has a suitable level of goodness-of-fit. But the intercept on *I* axes is almost zero, a result can be drawn that the reaction is mainly controlled by the mass transfer [29, 35-37]. Stirring could enhance the solute advection-diffusion, which can improve ions adsorbing on the surface of the working electrode and β-PbO_2 electrodeposition. Therefore the surface concentration of the intermediate product is determined by the transport of Pb^{2+} supplied to the electrode [29].

Fig.9 shows the Steady-state polarization curve of the Pt-RDE for the solution: 15 g/L HNO_3+30 g/L $Co(NO_3)_2 \cdot 6H_2O$+200 g/L $Pb(NO_3)_2$. The steady-state current density increases as the working electrode potential grows gradually from 1.3 V to 1.8 V. The current density remains stable at the potential range of 1.4~1.6 V, which is about 6 mA/cm^2, indicating that β-PbO_2-CoO_x deposition process is mainly controlled by electrochemical at potentials lower than 1.4 V and mainly controlled by mass transfer at potentials more than 1.4 V. When the potentials are more than 1.6 V the current density has a sharp rise, corresponding to the oxygen evolution. Therefore, in order to avoid concentration polarization and oxygen evolution to get the maximum amount of β-PbO_2, so the current

density should be controlled at 6 mA/cm^2. Then the stable β-PbO_2 deposition can be obtained. The process of Co-doped PbO_2 electrodeposition on the surface of RDE is shown in Fig. 10.

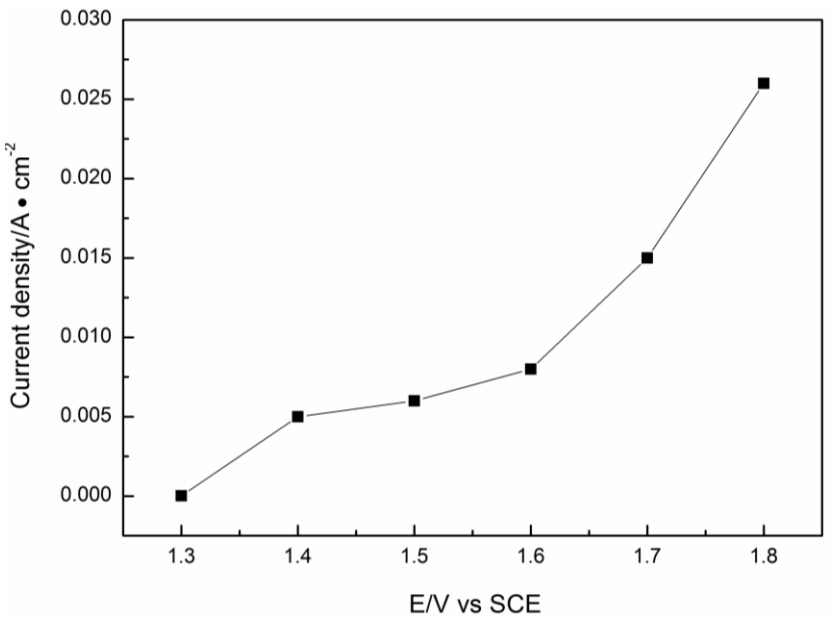

Figure 9. Steady-state polarization curve of the Pt-RDE for in 15 g/L HNO_3+30 g/L $Co(NO_3)_2 \cdot 6H_2O$+200 g/L $Pb(NO_3)_2$

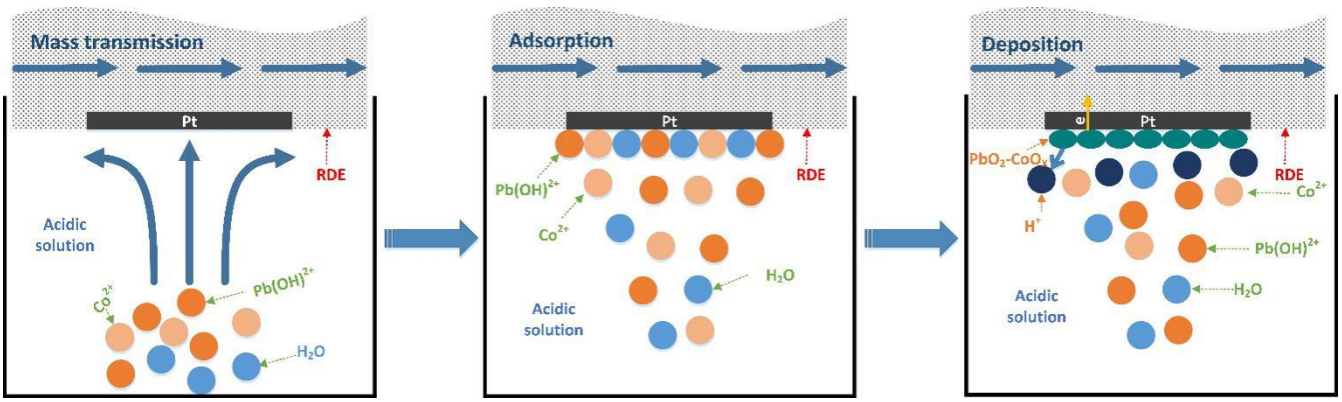

Figure 10. Schematic diagram of the Co-doped lead dioxide electrode position process on RDE surface

3.3. Phase compositions and surface microstructures

Fig. 11 shows the SEM patterns of β-PbO_2 and β-PbO_2-CoO_x. As can be seen, β-PbO_2 has similar morphology with Co-doped β-PbO_2-CoO_x, which is typically tetragonal rutile structure. Incorporation of cobalt into the β-PbO_2 film does not cause significant morphological change, which can also be observed in reference [18]. The β-PbO_2 deposits have block packing structure with larger grain. Compared with pure β-PbO_2, the deposits obtained from the solution with Co^{2+} presence has better oriented crystals, most of crystals have octahedral structure and lower size, the similar

conclusion was obtained in reference [38]. The different deposition overpotential of β-PbO_2 and β-PbO_2-CoO_x may able to explain the result of Co^{2+} lowering the crystal size of the β-PbO_2-CoO_x deposites.

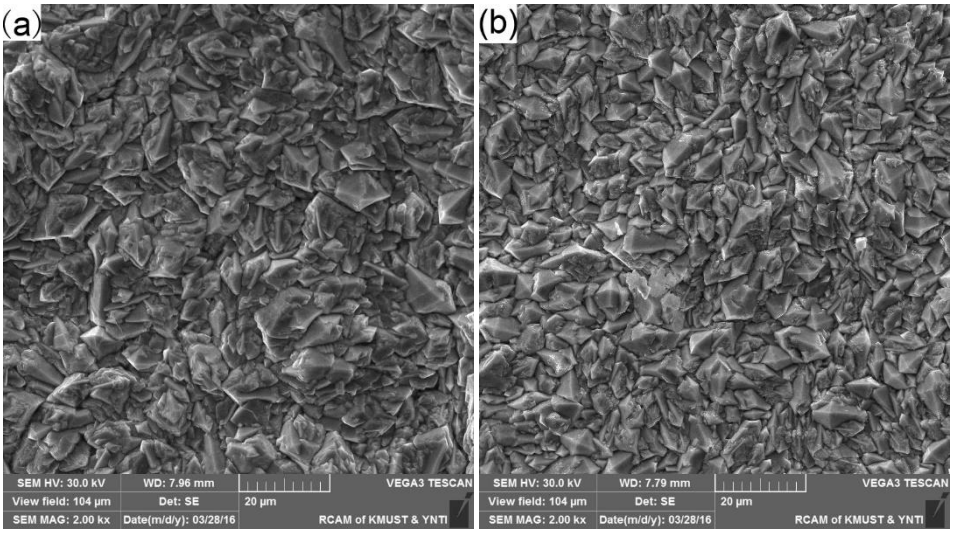

Figure 11.SEM images of PbO_2 deposited on the Pt-RDE in solutions: a, 15 g/L HNO_3+200 g/L $Pb(NO_3)_2$; b, 15 g/L HNO_3+30 g/L $Co(NO_3)_2 \cdot 6H_2O$+200 g/L $Pb(NO_3)_2$ at 30 ℃

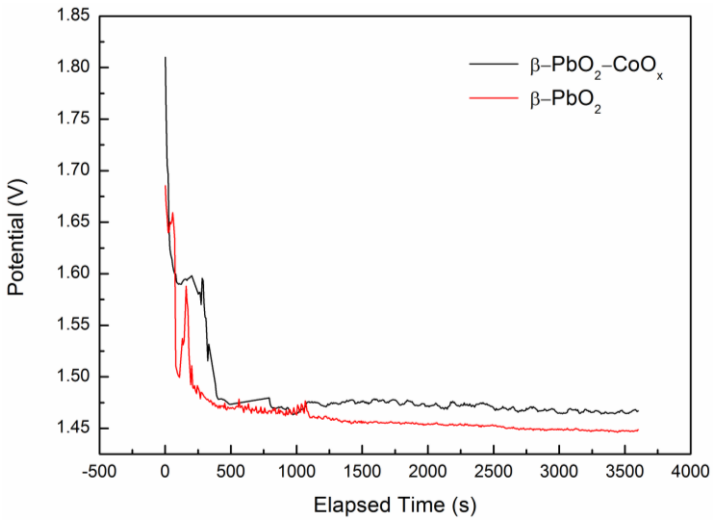

Figure 12. The E-t curves of the Pt-RDE at constant current for the solution: 1,15 g/L HNO_3+30 g/L $Co(NO_3)_2 \cdot 6H_2O$+200 g/L $Pb(NO_3)_2$; 2, 15 g/L HNO_3+200 g/L $Pb(NO_3)_2$ at 25 ℃

At 25 ℃, the anodic galvanostatic polarization behavior is tested under galvanostatic conditions, the constant current is 6 mA/cm^2. The anodic galvanostatic polarization process is shown in formula (3). E-t curve is shown in Fig. 12. The stable deposition potential of β-PbO_2 and β-PbO_2-CoO_x are about 1.44 V and 1.46 V. The equilibrium potential of the deposition process can be calculated from the Nernst equation in formula (4). Then the β-PbO_2 and β-PbO_2-CoO_x deposition

overpotential can be calculated from formula (5), the value are 2.902 V and 2.922 V, respectively. Apparently, adding Co^{2+} into the solution can enhance the β-PbO_2 deposition overpotential.

$$Pb^{2+} + 2H_2O \rightarrow PbO_2 + 4H^+ + 2e^- \qquad (3)$$

$$E = E^0 - \frac{RT}{nF}\ln Q \qquad (4)$$

In the equation, E is the equilibrium potential, E^0 is the Standard potential, R is Gas constant (8.314 $J \cdot k^{-1} \cdot mol^{-1}$), T is the temperature, n is the number of electrons obtained and lost in the electrode reaction, F is the Faraday constant (96.5×10^3 $C \cdot mol^{-1}$). Q is the activity quotient of product and reactant.

$$\eta_k = \eta - E \quad (5)$$

In the equation, η_k is the deposition overpotential, η is the stable deposition potential, E is the equilibrium potential.

According to the classic theory, the nucleation power of the metal ions on the electrode surface:

$$A = \frac{32\sigma^2 v^2}{n^2 F^2 \eta_k^2} \quad (6)$$

In the equation, A is the nucleation power, η_k is the deposition overpotential, σ is surface tension, v is the molar volume of the crystals.

The relation between nucleation probability and overpotential:

$$W = B\exp\left(-\frac{b}{\eta_k^2}\right) \qquad (7)$$

In the equation, B and b are constant.

According to the two equations (6 and 7), the probability of nucleation is higher when the overpotential is higher. In this case, the quantity of new nucleation is larger, which is favourable for deposition as new core on the anode surface and refining the crystal particles of β-PbO_2, the similar analytical skill has been used in the papers written by R.D. Xu and V.H. Dodson [39,40]. A result can be drawn that incorporation of Co into the surface of β-PbO_2 gives rise to large amounts of nucleation points for β-PbO_2, which can shorten nucleation time, increase deposition rate and deposition amount of β-PbO_2. In the meantime, it also hampers the further growth of the β-PbO_2 crystals. As a result, the deposits obtained from the solution containing Co^{2+} have lower crystal size.

Fig. 13 shows the XRD patterns of β-PbO_2 and β-PbO_2-CoO_x synthesized on Pt electrode surface. The predominant crystalline phase of deposits is β-PbO_2 type, and there is not any other miscellaneous peak. Both undoped β-PbO_2 and Co-doped β-PbO_2 contain β-type and α-type crystal. It is unanimous with cyclic voltammetry curves previously reported that the PbO_2 film which electrodeposited from acidic solution is consisted of a mixture of α and β-PbO_2 crystallographic form, and the amount of α-form is few. The characteristic peaks of α-type exit at a diffraction angle 2θ=29°. In comparison with the case of Co-doped PbO_2, the undoped PbO_2 deposits has higher intensities of α-phase peak (α (111)) and lower peak intensities for the β (101), β (200) and β (301) planes, which was also observed inreference [41]. The Co-doped PbO_2 has no peak of α (002) and α (113). The peaks related to β-PbO_2 in Co-doped PbO_2 are more sharper than undoped PbO_2, indicating that a better degree of crystallinity of the Co-doped PbO_2, which confirms the SEM analysis above. Because the Co

content in the β-PbO_2-CoO_x is very few, peaks attributed to CoO_x have not been found. By the ICP-OES measurements, the Co content in the β-PbO_2-CoO_x composite coatings are about 0.0256 wt%.

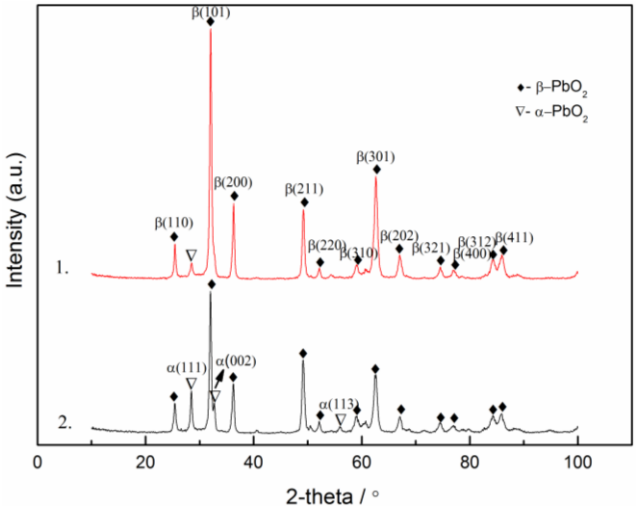

Figure 13. X-ray diffractograms of PbO_2 deposited on the Pt-RDE surface in solution: 1, 15 g/L HNO_3+30 g/L $Co(NO_3)_2 \cdot 6H_2O$+200 g/L $Pb(NO_3)_2$; 2, 15 g/L HNO_3+200 g/L $Pb(NO_3)_2$ at 30℃

4. CONCLUSIONS

In this research, the electrodeposition process of β-PbO_2-CoO_x from nitric acid solutions containing HNO_3, $Co(NO_3)_2 \cdot 6H_2O$ and $Pb(NO_3)_2$ has been examined by cyclic voltammetry and rotating disk electrode techniques. And the deposits are successfully obtained on the Pt surface under galvanostatic conditions. The increasing of $Co(NO_3)_2 \cdot 6H_2O$ concentration has a positive impact on electrodeposition of β-PbO_2 within the concentration range of 20~30 g/L, but a negative impact within the concentration range of 30~50 g/L. In addition, the rate and quantity of β-PbO_2 deposition increases at first then decreases, as $Pb(NO_3)_2$ concentration increases from 100 g/L to 200 g/L and at temperature range from 20 ℃ to 30 ℃. The suitable concentration of HNO_3 is 15 g/L. The amount of β-PbO_2 reaches to the maximum when the solution is consist of 15 g/L HNO_3, 200 g/L $Pb(NO_3)_2$ and 30 g/L $Co(NO_3)_2 \cdot 6H_2O$ at 30 ℃ (higher temperature is not welcome for PbO_2 deposition). In this Co^{2+} containing acidity solution, the β-PbO_2 deposition process is mainly controlled by the mass transfer. Steady-state polarization curve shows that β-PbO_2 deposition is mainly controlled by electrochemical when the potential is lower than 1.4 V and mainly controlled by mass transfer when the potential is higher than 1.4 V. The Co-doped PbO_2 has a more uniform morphology, smaller crystal size and better degree of crystallinity than pure PbO_2. In addition, Co^{2+} added to the solution can advance the formation of β-PbO_2 and interfere with process of α-PbO_2 deposition.

ACKNOWLEDGEMENT
Authors gratefully acknowledge the financial supports of the Key Project of Yunnan Province Applied Basic Research Plan of China (Project No.2014FA024); the National Natural Science Foundation of China (Project No.51564029); the Specialized Research Fund for the Doctoral Program of the Ministry of Education of China (Project No.20125314110011).

References

1. S. Rashkov, T. Dobrev, Z. Noncheva, Y. Stefanov, B. Rashkova, and M. Petrova, *Hydrometallurgy,* 52 (1999) 2230
2. R. Amadelli, A.D. Battisti, D.V. Girenko, S.V. Kovalyov, and A.B. Velichenko, *Electrochim.Acta,* 46, (2000) 341
3. J. Wu, H. Xu and W. Yan, *RSC Adv*., 25(2015) 19284
4. D. Velayutham and M. Noel, *J. Appl. Electrochem*.,23 (1993) 922
5. Y. Samet, S.C. Elaoud, S. Ammar, and R. Abdelhedi, *Journal of Hazardous Materials,* 138, (2006) 614
6. D.C. Johnson and J. Feng, L.L. Houk, *Electrochim. Acta,* 46,323 (2000)
7. H. An, Q. Li, D.Tao, H. Cui, X. Xu, L. Ding, and J. Zhai, *Appl. Surf. Sci.,* 258 (2011) 218
8. J. Xing, D. Chen, W. Zhao, X. Zhao, and W. Zhang, *RSC Adv.,* 66 (2015) 53504
9. W. Yang, and X. Lin, Appl. *Surf. Sci.,* 258, (2012) 5716
10. W. Zhang, H. Lin, H. Kong, H. Lu, Z. Yang, and T. Liu, Int. *J, Hydrogen Energy,* 39 (2014) 17153
11. C.J. Yang and S.M. Park, *Electrochim. Acta,* 108 (2013) 86.
12. W. Mindt, *Journal of Electrochemcal Society,* 116 (1969) 1076.
13. B.A. Sexton, G.F. Cottenrill, and S.F. letcher, *Journal of Vacuum Science & Technology A,* 8 (1990) 544
14. C.A. Gervasi, J.R. Vilche, and E. Alvarez, *Electrochim. Acta,* 41 (1996) 455
15. E. Keshavarz Alamdari, D. Darvishi, M. Samadi Khoshkhoo, F.A. Javid, S.P.H. Marashi, *Hydrometallurgy,* 119-120 (2012) 77
16. S. Cattarin, I. Frateur and P. Guerriero, etal, *Electfochim. Acta,* 45 (2000) 2279
17. D.F.A. Koch, *Australian J. chem.,* 12 (1959) 127
18. A.B. Velichenko, R.Amadelli, E.A. Baranova, D.V. Girenkoand F.I.D anilov, *Journal of Electroanalytical.,*527 (2002) 56
19. K. Polat, M.L. Aksu, and A.T. Pekel, *J. Appl. Electrochem.,* 32 (2002) 217
20. R. Wartena, J. Winnick, and P.H. Pfromm, *J. Appl. Electrochem.,* 32 (2002) 725
21. J.M. Maciel and S.M.L. Agostinho, *J. Appl. Electrochem.,* 30 (2000) 981
22. J.O.M. Bockris and A.K.N. Reddy, *Electrochim. Acta,* 22 (1977) 41
23. A.J. Bard and L.R. Faulkner, Electrochemical Methods: *Fundamentals and Applications,* Wiley, New York (2001).
24. G. Prentice, *Electrochemical Engineering Principles,* Prentice Hall (1991).
25. A. Neville, T. Hodgkiess, and A.P.Morizot, *J. Appl. Electrochem.,* 29, (1999) 455
26. H.Chang and D.C.Johnson, *J.Electrochem.Soc.,*136(1989)17
27. B.M. Chen, Z.C Guo, and X.W. Yang, *China Nonferrous Metallurgy,*2 (2009) 54
28. A.B. Velichenkoa, R. Amadellib, E.V. Gruzdevaa, T.V. Luk'yanenkoa, and F.I. Danilova, *Journal of Power Sources,* 191 (2009) 103
29. A.B. Velichenko, D.V. Girenko, and F.I. Danilov, *J. Electroanal. Chem.,* 405 (1996) 127
30. M. Jozegholami, A.N. Nikoloski, *Hydrometallurgy,*129-130 (2012) 59
31. F.I. Danilov,A.B. Velichenko, L.N. Nishcheryakova, *Electrochim. Acta,* 39 (1994) 1603
32. A.B. Velichenko, D.V. Girenko, and F.I. Danilov, *Russ. J.Electrochem.,* 33 (1997) 96

33. A.B. Velichenko, E.A. Baranova, D.V. Girenko, R. Amadelli, and F.I. Danilov, *Russ. J.Electrochem*, 39 (2003) 615
34. A.B. Velichenko and D. Devilliers, *J. Fluorine. Chem.*, 128 (2007) 269
35. F.B rusciotti and P. Duby, *Electrochim. Acta*, 52 (2007) 6644
36. T.D. Cabelka, D.S. Austin and D.C. Johnson, *J. Electrochem. Soc.*, 131 (1984) 1595
37. A.B. Velichenko, D.V. Girenko and F.I. Danilov, *Electrochemical. Acta*, 40 (1995) 2803
38. H.T. Yang, B.M. Chen, J.H. Liu, Z.C. Guo, Y.C. Zhang, R.D. Xu, *Rare Metal Materials and Engineering*, 43 (2014) 2889
39. R.D. Xu, L.P. Huang, J.F. Zhou, P.Zhan, Y.X. Guan, Y.Kong, *Hydrometallurgy, 125–126 (2012) 8*
40. Y. Jin, F.W. Wang, M. Xu, Y.H. Hun, W.Y. Fang, Y.J. Wei, C.J. Zhu, *Journal of the Taiwan Institute of Chemical Engineers*, 51 (2015) 135
41. V.H.Dodson, *J. Electrochem. Soc.*,101 (1961) 401